132 *Chem. Mater.* **2011,** *23,* 132–136
DOI:10.1021/cm101938e

CHEMISTRY OF MATERIALS
Article

One-Pot Synthesis of Pt Nanocubes and Nanopods via Burst Nucleation and Controlled Secondary Growth

Max N. Mankin, Vismadeb Mazumder, and Shouheng Sun*

Department of Chemistry, Brown University, Providence, Rhode Island 02912, United States

Received July 12, 2010. Revised Manuscript Received October 3, 2010

We report a one-pot solution-phase synthesis of Pt nanocubes and nanopods by adjusting the reaction time between 1 and 15 min. The nanocubes were synthesized in 1 min by controlled burst nucleation of Pt in the presence of low boiling point solvents hexane and acetone, while nanopods were obtained in 15 min via the secondary growth of polyhedral particles on the vertices of the existing Pt nanocubes in the presence of *N*-methylpyrrolidone. The Pt nanostructures were characterized by transmission electron microscopy, powder X-ray diffraction, and cyclic voltammetry. The nanocubes are dominated by (100) facets while the nanopods have more (111) character. The burst nucleation and secondary growth mediated by hexane/acetone and *N*-methylpyrrolidone may lead to new, or more easily synthesized, morphologies of Pt and other transition metal nanostructures.

Introduction

Synthesis of Pt nanoparticles (NPs) with controlled size and morphology has drawn enormous interest because their catalytic activity toward reactions key to chemical energy conversion, including methanol or carbon monoxide oxidation[1] and oxygen reduction,[2,3] is often NP size and shape dependent. Given the ever increasing demand on Pt usage and limited Pt reserves, one of the necessary approaches to future sustainability of Pt catalysis lies in decreasing the catalyst's Pt loading through efficiency (i.e., activity) increases.[4−6] One way forward is through shape control of Pt NPs, as catalysis kinetics can be controlled and optimized via the faceted nanocrystals.[7,8] Great efforts have been made in synthesizing and understanding growth mechanisms of Pt NPs of various morphologies in the hopes of enhancing their catalytic effectiveness. Studies of Pt NP growth via Pt deposition on existing Pt NPs have indicated that growth usually occurs on Pt(111) crystal facets to yield (100)-dominated NPs but depends primarily on the presence of a capping ligand.[9] This preferential growth on Pt(111) is also seen in the synthesis of Pt nanocubes where Pt nuclei, formed initially as octopods, grew into cubes.[10,11] Alternatively, the shape of the Pt NPs can be controlled either by trace amounts of an iron species and oxygen to retard the reduction of Pt^{2+} to Pt^0 in the polyol synthesis[12] or by adding a small amount of $Fe(CO)_5$ to mediate the Pt nucleation and growth into cubes.[7] Moreover, silver has been shown to induce particle nucleation and to control the face on which Pt deposits to achieve cubes, cuboctahedra, octahedra, and multipods.[13,14] In these syntheses, reactant concentration and reaction time are the common variables applied to achieve Pt NP shape control. Further catalytic studies on oxygen reduction in H_2SO_4 showed that the 7 nm Pt nanocubes having primarily Pt(100) facets were more active than 3 nm polyhedral and 5 nm cuboctahedral NPs, indicating the dominant effect of particle morphology over particle size.[7]

Here, we report a new procedure leading to Pt nanocubes and nanopods via burst nucleation followed by controlled growth of Pt. Burst nucleation causes the formation of nuclei from a supersaturated solution of monomers.[15,16] The initial nucleation event reduces the local concentration of monomers in the solution below supersaturation, prohibiting more nuclei from forming.[17] Then, the nuclei undergo diffusional growth as monomers

*To whom correspondence should be addressed. E-mail: ssun@brown.edu.

(1) Lee, S. W.; Chen, S.; Sheng, W.; Yabuuchi, N; Kim, Y.-T.; Mitani, T.; Vescovo, E.; Shao-Horn, Y. *J. Am. Chem. Soc.* **2009**, *131*, 15669–15677.
(2) Rolison, D. *Science* **2003**, *299*, 1698–1701.
(3) Ye, H.; Crooks, R. M. *J. Am. Chem. Soc.* **2005**, *127*, 4930–4934.
(4) Zhang, J.; Vukmirovic, M. B.; Xu, Y.; Mavrikakis, M.; Adzic, R. R. *Angew. Chem., Int. Ed.* **2005**, *44*, 2132–2135.
(5) El-Deab, M. S.; Ohsaka, T. *Angew. Chem., Int. Ed.* **2006**, *45*, 5963–5966.
(6) Chalk, S. *DOE Hydrogen Program Review*, 2004.
(7) Wang, C.; Daimon, H.; Lee, Y.; Kim, J.; Sun, S. *J. Am. Chem. Soc.* **2007**, *129*, 6974–6975.
(8) Markovic, N. M.; Gasteiger, H. A.; Ross, P. N., Jr. *J. Phys. Chem.* **1995**, *99*, 3411–3415.
(9) Petroski, J. M.; Wang, Z. L.; Green, T. C.; El-Sayed, M. A. *J. Phys. Chem. B* **1998**, *102*, 3316–3320.
(10) Ren, J.; Tilley, R. D. *J. Am. Chem. Soc.* **2007**, *129*, 3287–3291.
(11) Cheong, S.; Watt, J.; Ingham, B.; Toney, M. F.; Tilley, R. D. *J. Am. Chem. Soc.* **2009**, *131*, 14590–14595.
(12) Chen, J.; Herricks, T.; Xia, Y. *Angew. Chem., Int. Ed.* **2005**, *44*, 2589–2592.
(13) Teng, X.; Yang, H. *Nano Lett.* **2005**, *5*, 885–891.
(14) Song, H.; Kim, F.; Connor, S.; Somorjai, G. A.; Yang, P. *J. Phys. Chem. B* **2005**, *109*, 188–193.
(15) Shore, J. D.; Perchak, D.; Shnidman, Y. *J. Chem. Phys.* **2000**, *113*, 6276–6284.
(16) Robb, D. T.; Privman, V. *Langmuir* **2008**, *24*, 26–35.
(17) LaMer, V. K.; Dinegar, R. J. *J. Am. Chem. Soc.* **1950**, *72*, 4847–4854.

Published on Web 12/20/2010

from the surrounding solution attach to them.[17] Such monomer attachment/diffusional growth often follows standard crystal growth models. This two stage nucleation−growth model has been theoretically shown to produce spherical NPs.[18−25] Recent work by Gorshkov et al. simulated the evolution of face-centered cubic (fcc)-structured nuclei into shaped NPs and confirmed what had been previously observed experimentally about preferential Pt addition on (100) faces to yield (111) dominated Pt NPs.[26] Experimentally, burst nucleation has produced catalytically active, monodispersed Au, Pd, and Ni NPs between 2 and 10 nm sizes.[27−30] In these instances, the burst nucleation was triggered by borane reduction of metal precursors, leading to polyhedral NPs surrounded by low energy (111) facets.[31−33]

In our synthesis, the burst nucleation was initiated by fast reduction of $Pt(acac)_2$ (acac = acetylacetonate) with a morpholine borane (MB) complex in the presence of *N*-methyl-2-pyrrolidone (MP), hexane, and acetone. Oleylamine (OAm) served both as solvent and surfactant. The synthesis yielded 10−12 nm Pt nanocubes in just 1 min. Longer reaction time promoted further nucleation and growth of Pt on the corners of the existing Pt nanocubes, producing Pt nanopods. The proposed pathway leading to cubic and pod shapes was confirmed by transmission electron microscopy (TEM) analyses of the NP samples obtained from various stages of the synthesis. Both the Pt nanocube and pod surfaces were differentiated using standard cyclic voltammetry (CV).

Experimental Section

Nanoparticle synthesis was performed in a standard airless Schlenk line setup and using commercially available reagents. Oleylamine (OAm; > 70%), morpholine borane (MB; 95%), *N*-methyl-2-pyrrolidone (MP; 99.5%), and $Pt(acac)_2$ (acac = acetylacetonate; 97%) were purchased from Sigma Aldrich. Hexanes and acetone were purchased from Mallinckrodt Baker, Inc. Samples for TEM analysis were prepared by depositing one drop of diluted NP dispersion in hexane on amorphous carbon coated copper grids. Images were obtained by a Philips EM 420 (120 kV). High resolution transmission electron microscopy (HRTEM) images were obtained on a JEOL 2010 TEM (200 kV). X-ray diffraction (XRD) patterns were obtained on a Bruker AXS D8-Advanced diffractometer with Cu Kα radiation ($\lambda = 1.5418$ Å). Electrochemical measurements were performed on a Pine Electrochemical Analyzer, Model 701A, ALS/[H] CH Instrument by a typical, rotating disk electrode CV technique.

In a typical synthesis, 1 mmol of MB was dissolved in 16 mL of OAm at room temperature. The solution was stirred vigorously by a magnetic stirrer and heated at 3 °C/min to 50 °C under nitrogen flow. Once the MB was dissolved around this temperature, the stirring was stopped to maximize micelle formation.[34,35] The reaction solution was heated to 120 °C, and a solution of 0.075 mmol of $Pt(acac)_2$ in 2 mL of OAm, 1 mL of MP, 1 mL of hexane, and 1 mL of acetone prepared at room temperature was injected at this temperature. The reaction solution changed from colorless to yellow. Just after the injection, the solution temperature dropped to 115−117 °C but climbed back to 120 °C after 1 min when the solution became brown. The solution continuously darkened to deeper brown over the next several minutes. To isolate Pt nanocubes, the reaction mixture was quenched using an ice water bath exactly 1 min after injection of the Pt precursor solution. Otherwise, Pt nanopods were isolated after 15 min. The reaction mixture was cooled down to room temperature, and 45 mL of ethanol was added. The resultant brown mixture was centrifuged at 8000 rpm. The supernatant was discarded, and the solid product was collected and redispersed in hexane. One milliliter aliquots were taken by a syringe through a rubber septum into the reaction flask (the syringe was prepurged with nitrogen). These extractions were worked up with the same ethanol/centrifugation technique but on a smaller scale.

For electrochemical measurements, the Pt NPs were dispersed in hexane and then mixed with Ketjan Black carbon support with mass equal to the NPs. The suspension was sonicated for an hour to ensure the NP attachment to the carbon supports. The NP−carbon mixture was treated with glacial acetic acid at 75 °C for 6 h to remove surfactants from the particles. The suspension was centrifuged, and the NPs on carbon support were resuspended in distilled water at a concentration of 2 mg Pt+C/mL. Twenty microliters of the 2 mg Pt+C/mL aqueous dispersion was deposited onto a polished rotating disk electrode (RDE). The water was evaporated under low vacuum conditions; 20 μL of 0.1 M nafion solution was placed on top of the NP−carbon deposit, and water was removed. The RDE was submerged in a 0.1 M $HClO_4$ electrolyte solution with constant nitrogen bubbling. Ag/AgCl and Pt wires were used as reference and counter electrodes, respectively. The potential was scanned from −250 to 1000 mV. CV curves were measured at scan rates of 20 to 50 mV/s to measure hydrogen (H)-adsorption.[36]

Results and Discussion

TEM studies were conducted on the products obtained in the above reaction. Figure 1a is a low-resolution TEM image of a typical product separated from the reaction mixture after 1 min. The 10−12 nm NPs are cubelike. High resolution TEM (HRTEM) studies show that these

(18) Robb, D. T.; Halaciuga, I.; Privman, V.; Goia, D. V. *J. Chem. Phys.* **2008**, *129*, 184705-1–184705-11.
(19) Privman, V.; Goia, D. V.; Park, J.; Matijevic, E. *J. Colloid Interface Sci.* **1999**, *213*, 36–45.
(20) Libert, S.; Gorshkov, V.; Privman, V.; Goia, D.; Matijevic, E. *Adv. Colloid Interface Sci.* **2003**, *100−102*, 169–183.
(21) Privman, V. *Mater. Res. Soc. Symp. Proc.* **2002**, *703*, 577.
(22) Goia, D. V.; Matijevic, E. *Colloids Surf.* **1999**, *146*, 139–152.
(23) Libert, S.; Gorshkov, V.; Goia, D.; Matijevic, E.; Privman, V. *Langmuir* **2003**, *19*, 10679–10683.
(24) Park, J.; Privman, V.; Matijevic, E. *J. Phys. Chem. B* **2001**, *105*, 11630–11635.
(25) Mozyrsky, D.; Privman, V. *J. Chem. Phys.* **1999**, *110*, 9254–9258.
(26) Gorshkov, V.; Zavalov, A.; Privman, V. *Langmuir* **2008**, *25*, 7940–7953.
(27) Metin, O.; Mazumder, V.; Ozkar, S.; Sun, S. *J. Am. Chem. Soc.* **2010**, *132*, 1468–1469.
(28) Mazumder, V.; Sun, S. *J. Am. Chem. Soc.* **2009**, *131*, 4588–4589.
(29) Lee, Y.; Loew, A.; Sun, S. *Chem. Mater.* **2010**, *22*, 755–761.
(30) Peng, S.; Lee, L.; Wang, C.; Yin, H.; Dai, S.; Sun, S. *Nano Res.* **2008**, *1*, 229–234.
(31) Huang, X.; Zhang, H.; Guo, C.; Zhou, Z.; Zheng, N. *Angew. Chem., Int. Ed.* **2009**, *48*, 4808–4812.
(32) Wang, C.; Yin, H.; Chan, R.; Peng, S.; Dai, S.; Sun, S. *Chem. Mater.* **2009**, *21*, 433–435.
(33) Yin, Y.; Alivisatos, A. P. *Nature* **2005**, *437*, 664–670.
(34) Cushing, B. L.; Kolesnichenko, V. L.; O'Connor, C. J. *Chem. Rev.* **2004**, *104*, 3893–3946.
(35) Vriezema, D. M.; Aragonès, M. C.; Elemans, J. A. A. W.; Cornelissen, J. J. L. M.; Rowan, A. E.; Nolte, R. J. M. *Chem. Rev.* **2005**, *105*, 1445–1490.
(36) Biegler, T.; Rand, D. A. J.; Woods, R. *J. Electroanal. Chem.* **1971**, *29*, 269–277.

Table 1. Control Experiments Performed to Determine the Function of Hexane and Acetone in the Formation of the Pt Nanocubes

expt. no.	volume of alkane (mL)	volume of acetone or ketone (mL)	NP morphology after 1 min reaction (Figure)
1	0	0	monodisperse spherical (polyhedral) NPs (2a)
2	1	0	small random NPs (2b)
3	0	1	large random NPs (2c)
4	0.25	0.25	monodisperse NPs with some cubic character (2d)
5	1	1	cubes (1a)
6	2	2	polydisperse, aggregated NPs (temperature drop to 110 °C) (2e)
7	1 (pentane)	1	cubelike NPs (2f)
8	1 (pentane)	1	polydisperse cubes (2g)
9	1	1 (3-pentanone)	cubelike NPs (2h)

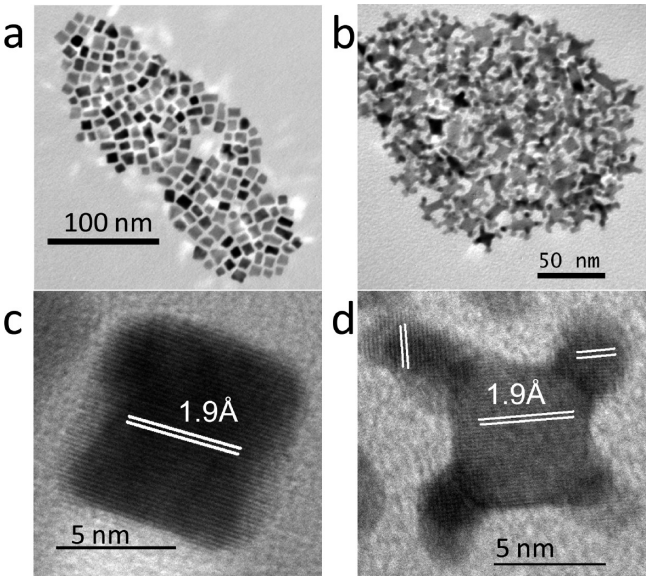

Figure 1. (a, c) Low and (b, d) high resolution TEM images of the 10−12 nm Pt nanocubes (a, b) and nanopods (c, d). White lines indicate lattice fringe spacing of 1.9 Å. Note that, in (d), the lattice fringes of the arms of the pods are not parallel to those of the central cube.

nanocubes have lattice fringes of ~1.95 Å (Figure 1b), corresponding to the interplane distance of (100) planes in fcc-Pt. These analyses indicate that, in the presence of MP, hexane, and acetone, the reduction of $Pt(acac)_2$ by MB led to fast nucleation and growth of Pt into cubes. After this 1 min of fast growth, the nanocubes become stable and show no further size increase. Instead, new nucleation and growth is observed after 15 min at the cube vertices, forming "nanopods" (Figure 1c), whose base nanocubes lie within the 10−12 nm range. HRTEM images of a typical Pt nanopod (Figure 1d) show the Pt's (100) (1.92 Å) that are either parallel or perpendicular to the (100) of the original seeding cube, indicating that the secondary Pt grows on (111) planes of the cube. Both Pt nanocubes and nanopods have the same crystal structure, as confirmed by X-ray diffraction (XRD) patterns of their assemblies (Figure S1, Supporting Information).

To study the factors that dominate the Pt growth in the current synthesis, we performed a series of control experiments by varying the reactants added in the reaction mixture and analyzed the Pt NP morphology at various synthetic stages. We found that MP was essential for Pt salt dissolution, and the presence of low-boiling point alkane/ketone solvents was vital to shape control. Table 1 summarizes the effect of alkane/ketone on the Pt NP

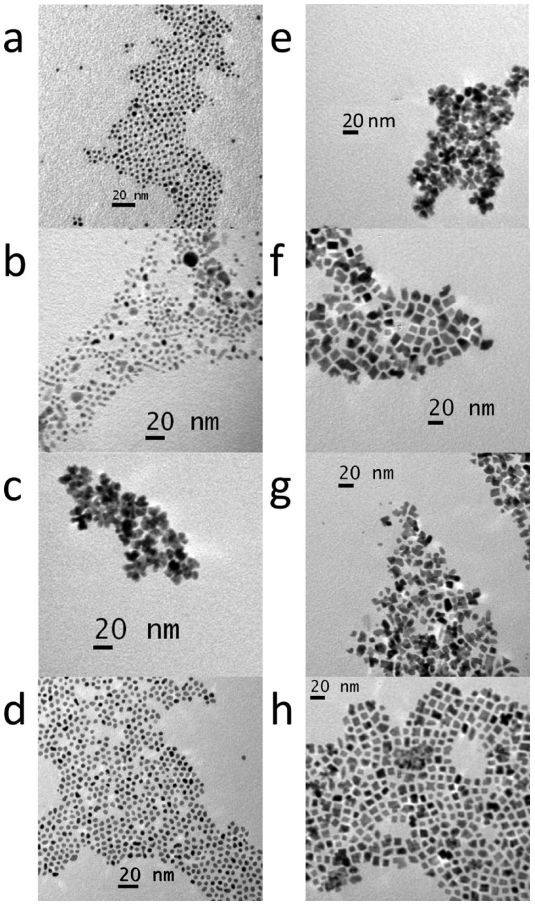

Figure 2. TEM images of the Pt NPs obtained from the experiments (a) 1, (b) 2, (c) 3, (d) 4, (e) 6, (f) 7, (g) 8, and (h) 9 in Table 1. All scale bars have been adjusted to 20 nm for easy comparison.

morphology, and Figure 2 shows TEM images of Pt NPs obtained from the experiments listed in Table 1. Without hexane and acetone in the injection solution (entry 1 in Table 1), Pt nanocubes could not be formed. Instead, the synthesis yielded spherical (or polyhedral) Pt NPs (Figure 2a). When only hexane or acetone was present in the reaction solution (entries 2 and 3 in Table 1), Pt NP size and morphology were difficult to control (Figure 2b,c), indicating that the combination of both hexane and acetone is necessary to form cubic NPs. In the case that hexane and acetone were injected in a small amount (0.25 mL; entry 4 in Table 1), Pt NPs with good size distribution were obtained, but Pt cubic shape was not well developed (Figure 2d). Too much hexane and acetone (each in 2 mL; entry 6 in Table 1) led to polydisperse and aggregated Pt NPs (Figure 2e). The presence of other alkanes and ketones (entries 7−9 in

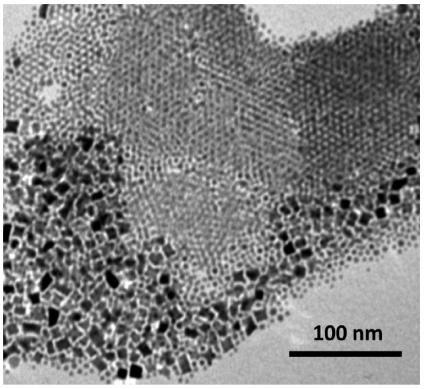

Figure 3. Typical TEM image of the mixture of Pt nanocubes and Pt NPs found in the aliquot taken from the reaction solution 5 min after the reaction at 120 °C. Some polyhedra attachment to cube corners is already visible.

Table 1) can also be used to make Pt with controlled shapes, although these Pt NPs had wider shape and size distributions (Figure 2f−h).

The unique shape control of Pt NPs in the current synthesis is apparently achieved using the low-boiling-point alkane and ketone solvents. When hexane and acetone are injected into the reaction mixture, these low boiling point solvents are evaporated quickly, leading to the drop of the solution's temperature to ~117 °C. At this temperature, the MB complex is still able to reduce Pt^{2+} and nucleation/growth within 1 min in the presence of trace acetone leads to the formation of Pt nanocubes. If too much (2 mL) hexane/acetone is injected, the solution temperature drops to ~110 °C. Increasing the reaction temperature from 110 °C back to 120 °C must cause multiple nucleation/growth events, leading to polydisperse Pt NPs (entry 6 in Table 1 and Figure 2e).

The Pt NP shape evolution in the presence of 1 mL of both hexane and acetone was monitored by taking aliquots of the reaction solutions at 1, 5, and 15 min and analyzing the morphologies of the Pt NPs separated from the sample solutions. As noted previously, nanocubes were synthesized after 1 min (Figure 1a). After 15 min of reaction, nanopods with smaller polyhedral NPs attached to the vertices of Pt nanocubes were obtained (Figure 1c), indicating growth on the corners of the cubic NPs, similar to what has been previously observed.[10] However, the aliquot at 5 min revealed two distinct morphologies present in solution: nanocubes and polyhedral NPs (Figure 3). This representative image shows that the particles are not actually growing at the cube corners, rather they grow as discrete entities in solution.

From what we observed during the synthesis, we hypothesize an alternative pod evolution mechanism to that seen previously, dependent on the fact that there exist two distinct periods of particle growth during the synthesis. While the Pt is nucleating throughout the duration of the synthesis, the manner of growth of those nuclei into particles depends on the presence of acetone (or another ketone). During the first minute, only a fraction of the Pt^{2+} is reduced to its zerovalent state by MB to form nuclei and cubes are formed in the secondary growth stage. This growth occurs in the presence of acetone, which has not yet been boiled off, as stated above. It is well accepted that the slowest growing crystal faces are the ones which appear on the surface of the crystal.[37] Here, the slowest growing face happens to be the (100) face which defines the majority of the surface of the nanocubes. As stated above, however, the Pt (111) face has been reported to be the slowest to grow during secondary growth of burst nuclei,[31−33] indicating that acetone prevents the growth of the (100) face, perhaps as a capping ligand, similar to what has been reported by El-Sayed et al.[9,38] Because growth on the (100) face is impeded, the (111) faces grow more easily, causing them to disappear and yield (100)-dominated cubes. Our result is contrary both to the aforementioned studies in which Pt (111) is the slowest to grow and to what has been shown by Gorshkov et al.,[26] who theoretically confirmed that the (100) face grows most rapidly in the secondary growth phase in fcc structured metals. Of course, the theoretical calculations did not account for the retardation of growth on the (100) face by acetone.

Over the next 4 min, more Pt^{2+} is reduced and more nuclei are formed, as indicated by the ongoing darkening of the reaction solution. By this point, the temperature of solution is stabilized at 120 °C, indicating that the hexane and acetone have been boiled off. Thus, the shape control provided by acetone is missing and polyhedral Pt NPs are formed because the (100) face is no longer capped, allowing the (100) face to grow and disappear. The resultant polyhedral product is seemingly identical to that obtained in the control experiment (entry 3, Table 1) without hexane and acetone and agrees with previous experimental and theoretical results in which the (100) face grows quickly to leave a (111) dominated NP.[26,31−33]

In the next 10 min, the (111) faceted polyhedral NPs attach to the remaining (111) vertices of the cubes, leading to the formation of nanopods through oriented attachment. This is seen in TEM images by the disappearance of both the stand-alone polyhedral NPs and the stand-alone cubic NPs in solution. Further evidence of this cube−particle attachment is found in the HRTEM images of the pods (Figure 1d), in which the lattice fringes of the cubes are misaligned with those of the attached particles. We attribute this oriented attachment to MP, which likely acts as a second capping surfactant on the (100) face. MP stabilizes the (100) faces, while attachment stabilizes the (111) faces. Thus, acetone guides the evolution of cubes during the second (growth) phase of burst nucleation while MP controls oriented attachment once the NPs are no longer growing. Such attachment also leads to a higher presence of (111)-faceted surfaces on the nanopods than the cubes, as the (111) faces on the polyhedral, which did not attach to the cubes, are still available.

Control experiments with Pd instead of Pt indicate that MP is vital to the formation of Pd nanopods as well. The

(37) Holden, A.; Singer, P. *Crystals and Crystal Growing*; Doubleday: New York, 1960.
(38) Ahmadi, T. S.; Wang, Z. L.; Green, T. C.; Henglein, A.; El-Sayed, M. A. *Science* **1994**, *272*, 1924–1926.

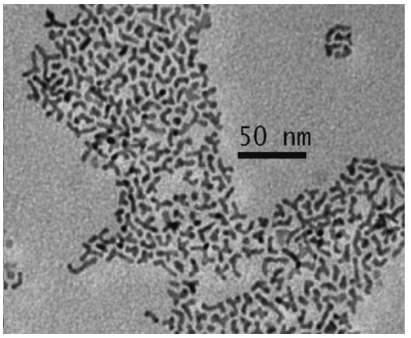

Figure 4. TEM images of the Pd nanopods synthesized via Pd burst nucleation in the presence of MP.

synthesis followed the same procedure as reported previously,[28] except oleylamine was replaced by MP. In this control synthesis, 10 mL of MP, instead of 10 mL of oleylamine, was added in the reaction mixture and Pd nanopods, not the polyhedral NPs as reported, were separated, as seen in Figure 4. Further experiments seem to indicate that the 5-member ring and amide bond present in the MP molecule are essential to the synthesis of these branched multipods, as the presence of 2-pyrollidone still produced Pd pods even though with poorer pod quality, while the presence of cyclopentanone or tetrahydrofuran led to the formation of polydisperse Pd particles with irregular shapes (Figure S2, Supporting Information).

The facets of both Pt nanocubes and nanopods were further characterized electrochemically by their hydrogen-(H)-adsorption curve in acid solution. Cyclic voltammograms (CV's) of the Pt nanocubes and nanopods in 0.1 M $HClO_4$ are shown in Figure 5. The differentiating electrochemical feature between the two morphologies is primarily the surface area of each kind of NPs, as calculated from H adsorption between approximately −0.2 and 0.1 V (vs Ag/AgCl). While the NP loading remained the same, the nanocubes' H adsorbing surface area is ~6.4 cm^2 and the nanopods' surface area is ~17.6 cm^2, further evidence of the cubes growth into pods with large surface area. Moreover, qualitative inspection of the two peaks in the H adsorption region reveals that the ratio between (100) and (111) surfaces is different between the two NP morphologies. The peak centered at −0.17 V corresponds to H adsorption on the (111) face and that at −0.1 V is due to the H adsorption on the (100) face.[39,40] The nanocubes display a more intense (100) peak while the nanopods show a higher (111) peak, further confirming that the polyhedra present in the pods contribute significant amounts of (111) facets to NP structure.

Conclusions

We have presented a novel and simple solution-phase burst nucleation synthesis of Pt nanocubes and nanopods.

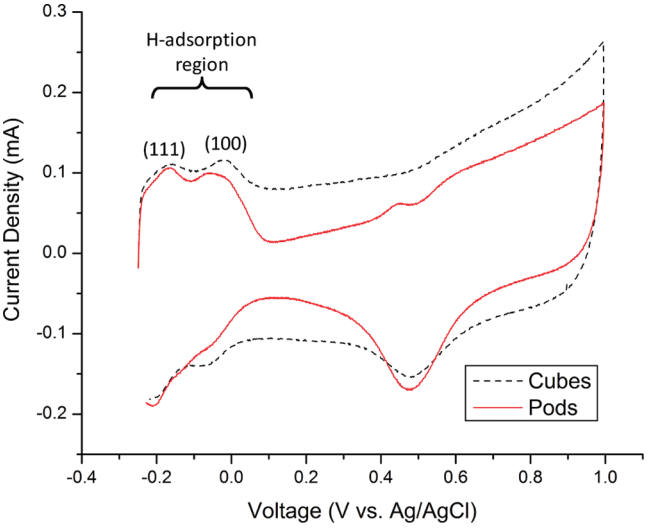

Figure 5. Cyclic voltammograms of the Pt nanocubes and the Pt nanopods in argon-saturated 0.1 M $HClO_4$ at room temperature. The rotating disk electrode rotated at 50 rpm, and the potential scan rate was at 50 mV/s. The cubes and pods display greater H adsorption on their (100) and (111) faces, respectively.

Hexane and acetone were employed to control the first growth phase of burst nucleation to produce Pt nanocubes in just 1 min. This reported nucleation and growth differs from what has been observed in previous theoretical and experimental studies of burst nucleation of fcc-structured noble metals. Once acetone boiled out of the solution, the secondary growth phase of burst nucleation yielded polyhedral NPs after 5 min. Unlike the previous growth in the presence of acetone, this growth is in agreement with previous studies which result in polyhedral NPs surrounded by low energy (111) facets. Due to the presence of *N*-methyl-2-pyrrolidone, nanopods were produced in 15 min via oriented attachment. The Pt NPs display unique, morphology-dependent surface structure consistent with what would be expected from their synthesis; the cubes' surfaces are dominated by (100) faces while the pods' surfaces have more (111) character. The principles involved in controlling the kinetics of burst nucleation and oriented attachment may lead to new, or more easily synthesized, morphologies of Pt and other transition metal nanostructures.

Acknowledgment. The work was supported in part by the U.S. Department of Energy, Office of Energy Efficiency and Renewable Energy, Fuel Cell Technologies Program. The authors thank Mr. Anthony McCormick for his assistance with HRTEM analysis.

Supporting Information Available: XRD patterns and additional TEM images of the nanostructures (PDF). This material is available free of charge via the Internet at http://pubs.acs.org.

(39) Ross, P. N. *Surf. Sci.* **1981**, *102*, 463–485.
(40) Markovic, M. N.; Ross, P. N. *Surf. Sci. Rep.* **2002**, *45*, 117–229.